

Effect of Metallic Inserts on the Strength of Pin Joints Prepared from Glass Fiber Reinforced Composites

Kulwinder Singh[#], J.S. Saini^{#,*}, and H. Bhunia[@]

[#]Mechanical Engineering Department, Thapar University, Patiala - 147 004, India

[@]Chemical Engineering Department, Thapar University, Patiala - 147 004, India

^{*}E-mail: jsaini@thapar.edu

ABSTRACT

The present study deals with the failure analysis of pin joints by varying different geometric parameters *i.e.*, edge distance to hole diameter (E/D) ratio and width to hole diameter (W/D) ratio. Pin joints were prepared from the glass fiber reinforced laminates incorporating the metal inserts. A range of 2 to 5 and 3 to 6 was considered for E/D and W/D ratios, respectively. The stress around the hole was redistributed by incorporating the metal inserts in the hole to increase the load carrying capacity. To predict the failure loads and failure modes numerically, progressive damage analysis along with Hashin failure criteria was used in the pin joints. Strength of the pin joints increased in the range of 65 per cent to 92 per cent with metal insert due to the redistribution of the stresses around the hole. Progressive damage analysis gave a good correlation with experimental findings. Thereafter, the strength of the joint was predicted by varying the thickness of the metal inserts.

Keywords: Glass fiber; Pin joints; Metal inserts; Progressive damage analysis; Hashin failure criteria

1. INTRODUCTION

To develop a light weight and high strength solutions for engineering problems, composite materials are being highly focused by number of industries these days. With huge applications in aircraft, marine, automotive, space, civil structures and sports industry, the fiber reinforced composites are in demand. Besides high strength to weight ratio, composite structures also exhibit a better dimensional stability.

For the real life applications, various components of machines or structures made from fiber reinforced composites need to be joined together. These composites can be joined with different mechanical or adhesive joining methods. In comparison to the adhesive joints, mechanical joints facilitate easy disassembly without destroying the basic components of the joint.

Various studies have been performed by different researchers on the mechanical joints for the effect of different parameters such as geometric ratios, material, fiber orientation, etc. Nilsson¹ proposed a method to increase the failure load in graphite-epoxy bolted joints by bonding a metallic insert in the hole. Herrera-Franco², *et al.* determined stress and strain distributions in single-pin lap joints prepared from glass epoxy laminate. The joints were analysed for hard and soft inserts. The results were compared with the specimens without the inserts. Rispler³, *et al.* proposed for change in the properties of highly stressed finite elements around a loaded hole in a stepwise evolutionary fashion, allowing the formation of an

insert. Camanho and Matthews⁴ incorporated adhesively bonded metallic inserts in the composite bolted joints. A 3D finite element model was developed to predict the damage in the laminate. Camanho⁵, *et al.* proposed a novel type of metallic insert with tapered ends, which resulted in delay in onset of damage in the composite. Use of bonded metallic inserts was investigated experimentally and numerically to increase the strength and the efficiency of single-shear composite bolted joints. Karakuzu⁶, *et al.* studied failure load, failure mode and bearing strength of a woven laminated glass-vinylester composite plate with single circular hole. Geometric variables *i.e.*, W/D and E/D ratios were taken into consideration for numerical and experimental results. Icten⁷, *et al.* investigated failure loads and the failure modes in mechanical joints prepared from woven Kevlar epoxy composite plates. Hashin, Hoffman and Maximum Stress criteria were used and their results were compared with each other. Baba⁸ discussed the effects of ply orientation, laminate edges and side distances on the strength of single pin joints. Karakuzu⁹, *et al.* investigated failure load, failure mode and bearing strength for the double pin joints. Two parallel rigid pins fitted into the laminate holes were subjected to a traction force. In addition to the experimental work, the failure modes and failure loads were obtained numerically using finite element methods along with the Hashin failure criteria. Karakuzu¹⁰, *et al.* investigated the effects of different geometric parameters on the failure modes and failure loads for the double pin joint in the serial configuration, experimentally and numerically. Atas¹¹ analysed bearing strength of the pin joints made from woven fabric having small weaving angles. Kishore¹², *et al.*

performed experimental and numerical investigations on multi-pin joints prepared from glass fibre/epoxy composite laminates. To predict the failure load and failure modes, finite element methods and Tsai–Wu failure criteria along with material property degradation was used in the numerical analysis. Aktas¹³, *et al.* analysed the single and double pin joints prepared from glass-epoxy composites for different geometric parameters. The numerical study was performed using ANSYS along with the Yamada-Sun failure criterion. Asi¹⁴ studied the effect of different geometric parameters on the strength of the single pin joints prepared from woven fabrics of different linear densities. Asi¹⁵ investigated the effect of Al₂O₃ particles on the bearing strength of single hole pin joints. Single-hole pin-loaded specimens with 7.5 wt. per cent, 10 wt. per cent, and 15 wt. per cent of the filler in the matrix were tested in tension. Karakuzu¹⁶, *et al.* studied the effects of hole positions on the failure mode and failure loads in three pin joints using different geometric parameters. Turan¹⁷, *et al.* carried out experimental and numerical work to predict the failure loads and failure modes for pinned joint prepared from carbon/epoxy composite plates. The effects of fiber orientation and joint geometry on the failure of pin joint was investigated. Finite element methods along with Hashin failure criteria was used to predict the failures numerically. Mara¹⁸, *et al.* incorporated metallic inserts in the hole and conducted experimental and finite element analyses to determine the effect of inserts on the bolt-tension relaxation, the stiffness and the load bearing behavior of joints. Singh¹⁹, *et al.* optimised geometric parameters for double pin joint in serial and parallel hole configurations using Taguchi method. For the numerical analysis, characteristic curve along with Tsai–Wu failure criterion was used to predict the bearing strength.

From the literature review it is seen that various parameters *i.e.*, E/D, W/D, P/D, Ply orientations and nano materials are important to improve the joint strength. It can also be seen that the behaviour of the joints can be improved by inserting a metal insert in the pin hole. The present work deals with the effect of metal insert on the strength of the pin joints.

2. EXPERIMENTATION

2.1 Materials

Epoxy, hardener, accelerator, glass fabric and metal inserts were used as different materials for preparation of pin joint specimens.

2.1.1 Resin

The DGEBA based epoxy resin (L-12), hardener (K-12) and accelerator (K-13), supplied by Atul Ltd., Guajrat India, were used in the present work. The modulus of elasticity, tensile strength, flexural strength and compressive strength for the supplied resin were 15-16 GPa, 70-90 MPa, 100-120 MPa, and 190-210 MPa, respectively²⁰.

2.1.2 Glass Fiber

The reinforcement material *i.e.*, Unidirectional E-glass fiber ‘Advantex’ of 1200 gsm was used in the present work. The material was provided by Owens Corning India Pvt. Ltd, Mumbai, India. The tensile strength, elastic modulus and

elongation at breaking load for single glass filament were 3100-3800 MPa, 80-81 GPa and 4.6 per cent, respectively²⁰.

The given properties of the resin and glass fiber are as per the technical data sheets supplied by the parent company.

2.1.3 Metal Insert

The inserts prepared from mild steel, as shown in Fig. 1, were press fitted into the specimens. The inner diameter (D_i) and outer diameter (D_o) of the metal insert were 4 mm and 6 mm, respectively. The height of the metal insert was same as the thickness of the specimens.

The density of the material was 7.87 g/cc. The tensile yield strength and young’s modulus of the metal insert material was 370 MPa and 205 GPa, respectively. The chemical composition of the material was, Iron (Fe) 98.8 per cent – 99.3 per cent, Phosphorous (P) ≤ 0.039 per cent, Sulfur (S) ≤ 0.049 per cent, Carbon (C) 0.15 - 0.19 per cent and Manganese (Mn) 0.61 per cent - 0.89 per cent.

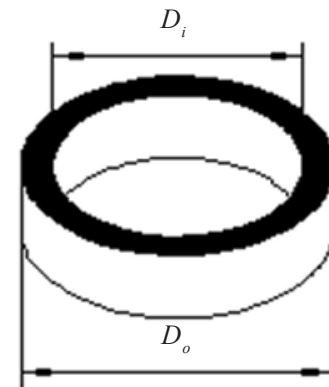


Figure 1. Geometry of the metal insert.

2.2 Laminate Processing and Mechanical Properties

Epoxy and glass fiber were used to prepare the composite laminates. Several methods are available for laminates preparation. Hand layup technique followed by compression moulding²⁰ was used in the present work. Followed by proper marking, glass fabric was cut into required size of the laminas with the help of a diamond cutter. To prepare the epoxy, all three components *i.e.*, resin, hardener and accelerator were mixed in the appropriate quantity and stirred well to obtain a homogenised mixture. The laminates were prepared layer by layer using hand lay-up technique with [0°/90°/0°] orientation. The epoxy to fiber weight ratio for the prepared laminate was 40:60 in the present work. Hand roller was used to remove air trapped in the laminate. The laminates were cured at room temperature (25 °C) for 24 h, followed by compression moulding. A force of 120 kN was applied at 180 °C temperature for 30 minutes followed by cooling to room temperature at the same force.

To determine the tensile modulus and tensile strength of the prepared laminates, specimens were tested on a Zwick-Roell Universal Testing Machine. The tests were conducted as per ASTM D3039 and D5379, respectively. Table 1 shows the different mechanical properties of the prepared glass epoxy composite laminates.

Table 1. Mechanical properties of the prepared laminates²⁰

Mechanical property	Symbol (units)	Value
Longitudinal modulus	E_1 (GPa)	12.8
Transverse modulus	E_2 (GPa)	7.8
Laminate shear strength	s (MPa)	155.68
Longitudinal strength in tension	X_t (MPa)	390.76
Transverse strength in tension	Y_t (MPa)	255.98
Poisson ratio	ν_{12}	0.32
Longitudinal strength in compression	X_c (MPa)	324.11
Transverse strength in compression	Y_c (MPa)	224.45

2.3 Pin Joint Configurations

In the present work, a plate (length L , width W , thickness t) with a single pin hole, as shown in Fig. 2, was used. The diameter, D , of the hole was fixed to 4 mm. A gradual increasing and uniform load was applied on the plate through a rigid pin inserted into the hole. The pin located at the center of the hole resists the applied load. Because of symmetry of the geometry and other boundary conditions about the center line of the specimen, no bending forces are present during tensile testing of the specimen. E/D and W/D ratios in the specimen were varied over the range of 2 to 5 and 3 to 6, respectively. Table 2 shows the different E/D and W/D ratios for which the samples were prepared.

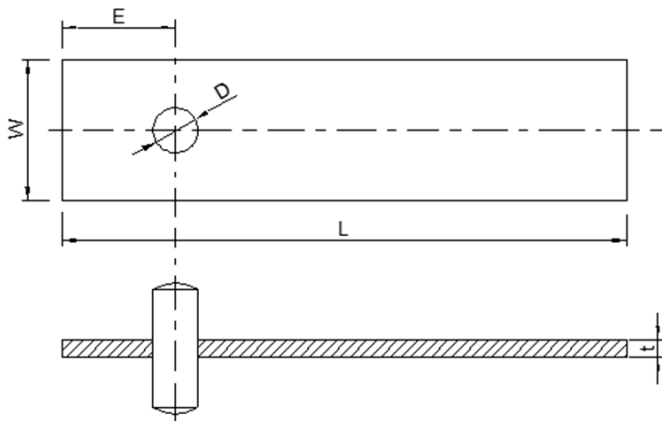


Figure 2. Geometry of the specimen without metal insert.

Table 2. Various values of E/D and W/D ratios

E/D	E (mm)	W/D	W (mm)	t (mm)	D (mm)
2	8	3	12	3	4
3	12	3	12	3	4
4	16	3	12	3	4
5	20	3	12	3	4
2	8	4	16	3	4
3	12	4	16	3	4
4	16	4	16	3	4
5	20	4	16	3	4
2	8	5	20	3	4
3	12	5	20	3	4
4	16	5	20	3	4
5	20	5	20	3	4
2	8	6	24	3	4
3	12	6	24	3	4
4	16	6	24	3	4
5	20	6	24	3	4

Thereafter, the metallic inserts were press fit into the holes of each of the specimens.

For the comparison of the strength of the specimens with and without the metal inserts, the inner diameter (D_i) of the metal inserts was taken as 4 mm which was same as the diameter (D) of the holes in the specimens without the metal inserts. The outer diameter (D_o) of the metal insert was of 6 mm. The geometric and the actual images of two specimens are shown in Figs. 3 and 4, respectively.

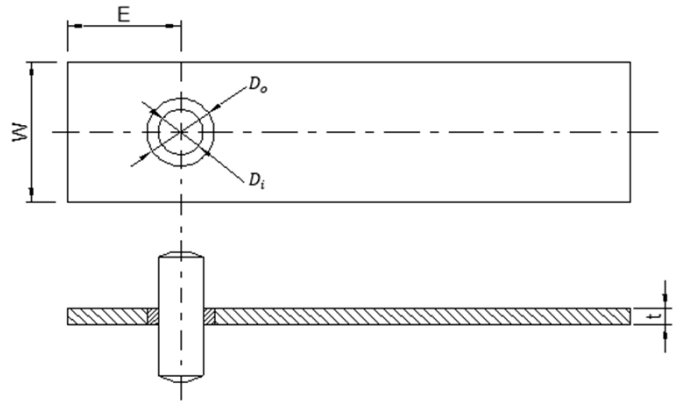


Figure 3. Geometry of the specimen with metal insert.

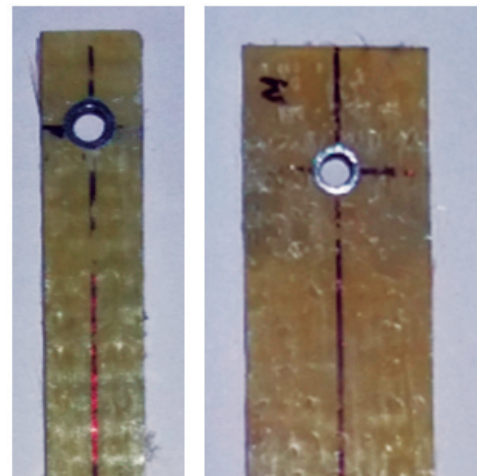


Figure 4. Metal inserts in specimens.

3. RESULTS AND DISCUSSIONS

To estimate the tensile strength, the laminates with and without the metal inserts were tested on universal testing machine (UTM) set to a crosshead speed of 2 mm/min. The metal inserts were press fitted into the drilled holes in the specimens. A rigid pin was inserted into the metal insert. The load was applied on the rigid pin through a metal fixture held in one of the grippers of the universal testing machine. The other side of the laminate was held on the second gripper of the universal testing machine.

Figure 5 shows the graphical plots for the force and the displacement variations for the specimens with and without the metal inserts. These plots are used to predict the type of failure mode in the specimens. There are three basic failure modes in pin joints *i.e.*, net-tension, shear-out and bearing²⁰. Joint failure with the shear-out and net-tension mode is immediate.

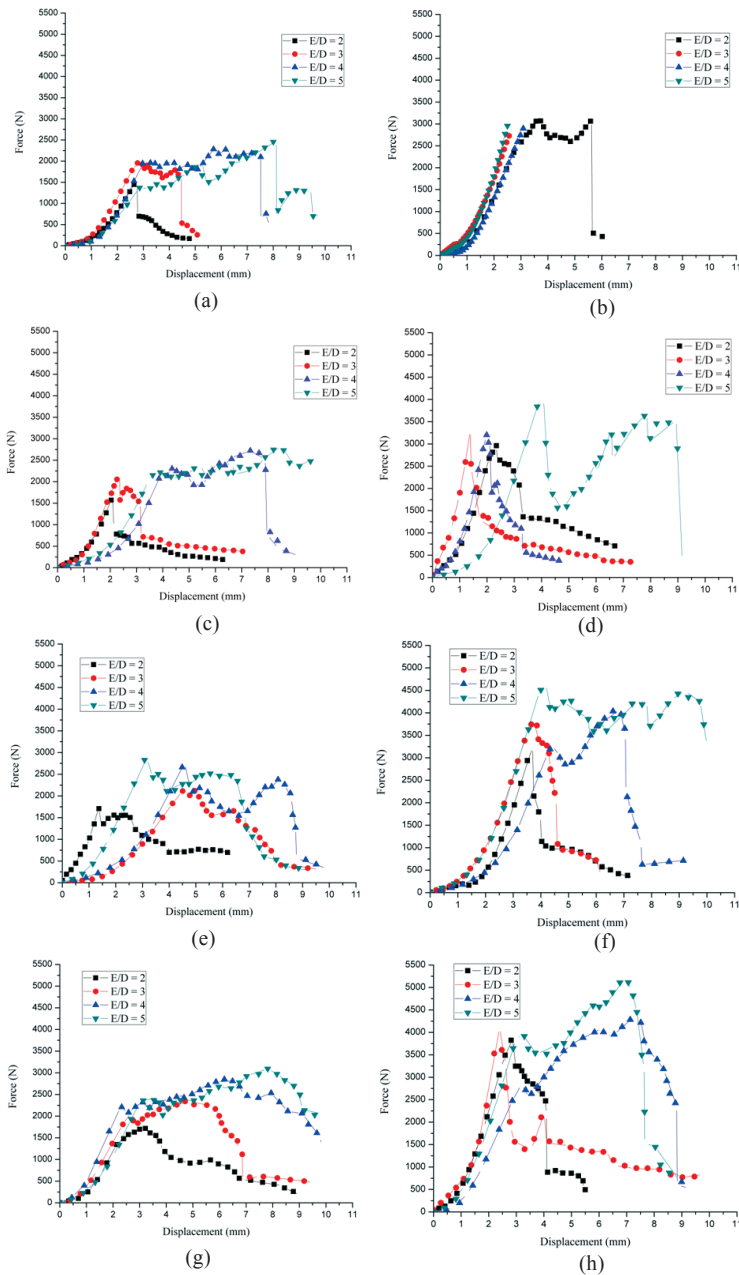


Figure 5. Load vs displacement graphs from the UTM tensile test for specimens with and without the metal inserts: (a) W/D = 3 (without insert), (b) W/D = 3 (with insert), (c) W/D = 4 (without insert), (d) W/D = 4 (with insert), (e) W/D = 5 (without insert), (f) W/D = 5 (with insert), (g) W/D = 6 (without insert), (h) W/D = 6 (with insert).

But the failure with the bearing mode is not sudden and have less serious consequences than the shear-out and net-tension types of failure modes. The designer avoids the net-tension and shear-out failure mode as compared to bearing failure modes²⁰. It can be seen from Fig. 5 that, at the lower values of W/D ratio, the specimens with metal inserts fail with net-tension mode as the distance of the metal insert to the side edge of the specimen is very small. The net-tension mode can be predicted from the instant drop in the graph. The failure mode of the specimens change from net-tension to the bearing failure mode with the increase in W/D and E/D ratios. The bearing failure mode can

be predicted from the multiple peaks in the graphs. It is also clear from Fig. 5 that the failure loads for specimen incorporating metal inserts are higher as compared to the specimens without metal inserts.

The ultimate failure loads for different joint configurations with and without metal inserts are as shown in Table 3. It is clearly observed from the table that the metal inserts have increased the failure load for each joint configuration. Similar trends have been reported for the bolt joint in previous study^{1,18}.

Table 3. Ultimate failure loads for various levels of E/D and W/D ratios

E/D	W/D	Failure loads (N)	
		No inserts	Metal inserts
2	3	1501	2890
3	3	2051	3000
4	3	2356	3100
5	3	2475	3010
2	4	1650	2960
3	4	2130	3300
4	4	2767	3346
5	4	2830	4010
2	5	1730	3243
3	5	2135	3850
4	5	2800	4100
5	5	2880	4640
2	6	1732	3850
3	6	2350	4105
4	6	2860	4351
5	6	3096	5205

Figure 6 shows the effect of E/D and W/D ratios on the ultimate failure loads for the specimens with and without the metal inserts. Figure 6 shows that the failure load for specimen with metal inserts having minimum configuration of E/D and W/D ratios as 2 and 3, respectively is 92 per cent larger as compared to the specimen without the metal inserts. Similarly, for the highest joint configuration of E/D and W/D ratios of 5 and 6, respectively, the failure load increases by 68 per cent for the specimen with metal insert in comparison to the specimen without the metal insert.

Table 4 summarises the failure modes for different pin joint configurations, where S, N and B signifies the shear-out, net-tension and bearing type of failure modes.

Introducing the metal inserts in the composite joint change the failure modes of the joints¹. Table 4 shows that for the lower values of W/D ratios, different failure mode *i.e.*, net-tension is observed for the specimens with the metal inserts as compared to the specimens without the metal inserts. It is due to the reason that the side edge to hole distance reduces for the lower value of W/D ratio. Although the failure load value is very high for lower value of W/D ratios but the lower value of W/D are to be avoided due to net-tension type of failure which is a catastrophic type of failure. The actual images for some of the specimens are as shown in Fig. 7.

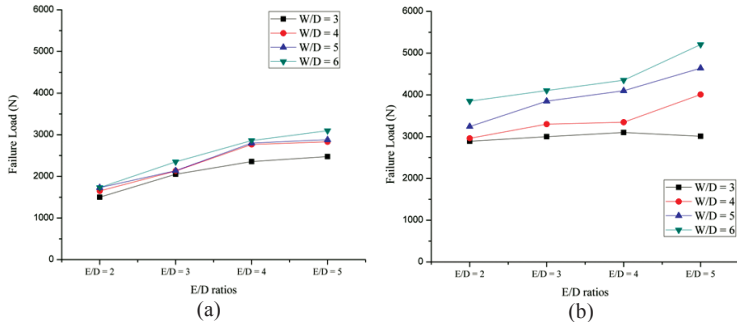


Figure 6. Ultimate failure load for the specimen (a) without metal inserts (b) with metal inserts.

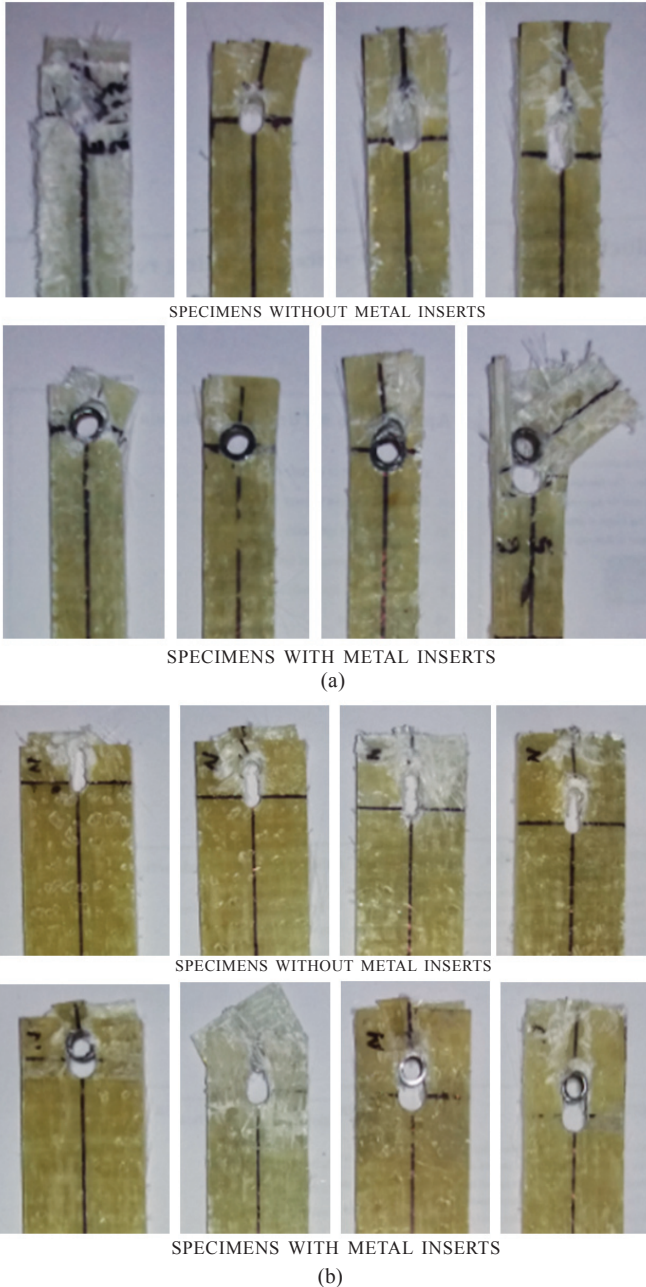


Figure 7. Failure modes of specimens with and without inserts, geometric parameters (a) E/D=2, W/D=3; E/D=3, W/D=3; E/D=4, W/D=3; E/D=5, W/D=3 and (b) E/D=2, W/D=6; E/D=3, W/D=6; E/D=4, W/D=6; E/D = 5, W/D=6.

Table 4. Failure modes for various levels of E/D and W/D ratios

E/D	W/D	Failure modes	
		No inserts	Metal inserts
2	3	S	N
3	3	S	N
4	3	B	N
5	3	B	N
2	4	S	S
3	4	S	S
4	4	B	S
5	4	B	B
2	5	S	S
3	5	S	S
4	5	B	B+S
5	5	B	B
2	6	S	S
3	6	B+S	S
4	6	B	B
5	6	B	B

4. NUMERICAL ANALYSIS

Commercial available software ANSYS has been used to perform finite element analysis of the composite joint specimen. The geometry, as shown in Fig. 2, was modeled in ANSYS modeler and then imported to ACP Pre-Module, where layer by layer composite definition was given to the model. Three layers with [0°/90°/0°] orientations and 1 mm thickness each were modeled. Mesh, as shown in Fig. 8, using a mapped face meshing technique with brick elements was generated.

As shown in Fig. 9, a 6000 N tensile force divided in 6 steps; starting from 0 and reaching up to 6000 N (max.), was applied onto the hole edge in longitudinal direction.

Hashin failure criteria²¹ using Eqns. (1) to (4) was used to perform the progressive failure analysis of the composite specimens.

Fiber failure used for tensile and compressive loadings in longitudinal direction (fiber direction) are given in Eqn. (1) and

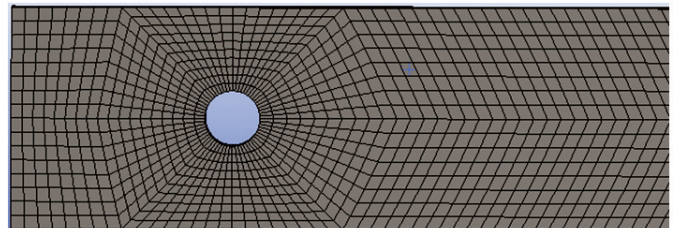


Figure 8. Generated mesh for a particular specimen.

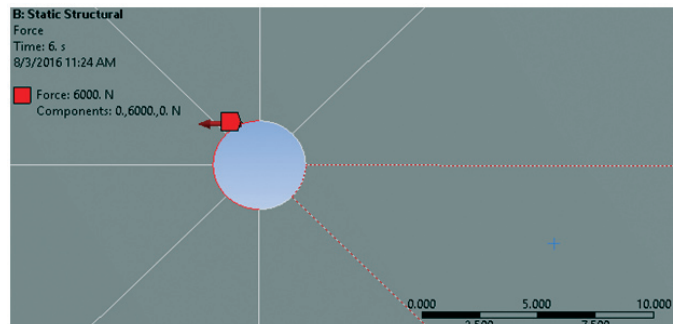


Figure 9. Tensile load applied on the hole boundary.

(2), respectively.

$$f_f = \left(\frac{\sigma_1}{X_t}\right)^2 + \left(\frac{\tau_{12}}{S}\right)^2, \sigma_1 \geq 0 \quad (1)$$

$$f_f = -\frac{\sigma_1}{X_c}, \sigma_1 < 0 \quad (2)$$

Fiber failure in compression in longitudinal (fiber) direction generally occurs due to buckling of the fiber. It is not sure that whether the shear components will weaken or strengthen the compressive strength in fiber direction²¹. Therefore, the shear terms are generally not considered in Eqn. (2).

Matrix failure for tensile and compressive loadings in transverse direction is given by Eqns. (3) and (4), respectively.

$$f_m = \left(\frac{\sigma_2}{Y_t}\right)^2 + \left(\frac{\tau_{12}}{S}\right)^2, \sigma_2 \geq 0 \quad (3)$$

$$f_m = \left(\frac{\sigma_2}{2S}\right)^2 + \left(\frac{\tau_{12}}{S}\right)^2 + \left[\left(\frac{Y_c}{2S}\right)^2 - 1\right] \frac{\sigma_2}{Y_c}, \sigma_2 < 0 \quad (4)$$

where f_f and f_m are the failure index for the fiber and the matrix, σ_1 and σ_2 are stresses in longitudinal and transverse directions, X_t and Y_t are tensile stress limits in longitudinal and transverse direction, respectively, X_c and Y_c are compressive stress limits in longitudinal and transverse direction, respectively and s is the in-plane shear stress.

During the progressive failure analysis, the load begins from the 0 value and increases gradually with small increments. Initially, failure begins in the middle layer which is known to be the first failure and it is mainly because of matrix compression. The reason behind early failure of the middle layer is the fiber orientations of 90° w.r.t. applied load. After middle ply failure, corresponding load initially taken by the middle layer is further distributed to outer layers *i.e.*, layer 1 and 3. Further increase of load causes last failure (outer layer failure) and the load corresponding to the last failure is significantly large compared to the first ply failure load. Fibers while being at 0° w.r.t. loading direction in 1st and 3rd layer are mainly responsible for carrying tensile loads in the outer layers.

Figure 10 shows the damage propagation for weakest joint configuration in the two outer layers *i.e.*, layers at 0° orientations with respect to the applied tensile load. As seen in Fig. 10, failure initially begins towards side edge but further propagates towards free edge and reach the free edge causing shear out failure.

Figures 10(a) and 10(b) shows that the damage initiates towards side edge around the hole surface and propagates further in the same direction. Figure 10(c) shows that the damage starts propagating towards free edge of the specimen and further approach free edge, confirming shear out failure mode of the specimen. The shear-out failure mode is due to the lesser margin between the free edge and the hole. Specimens

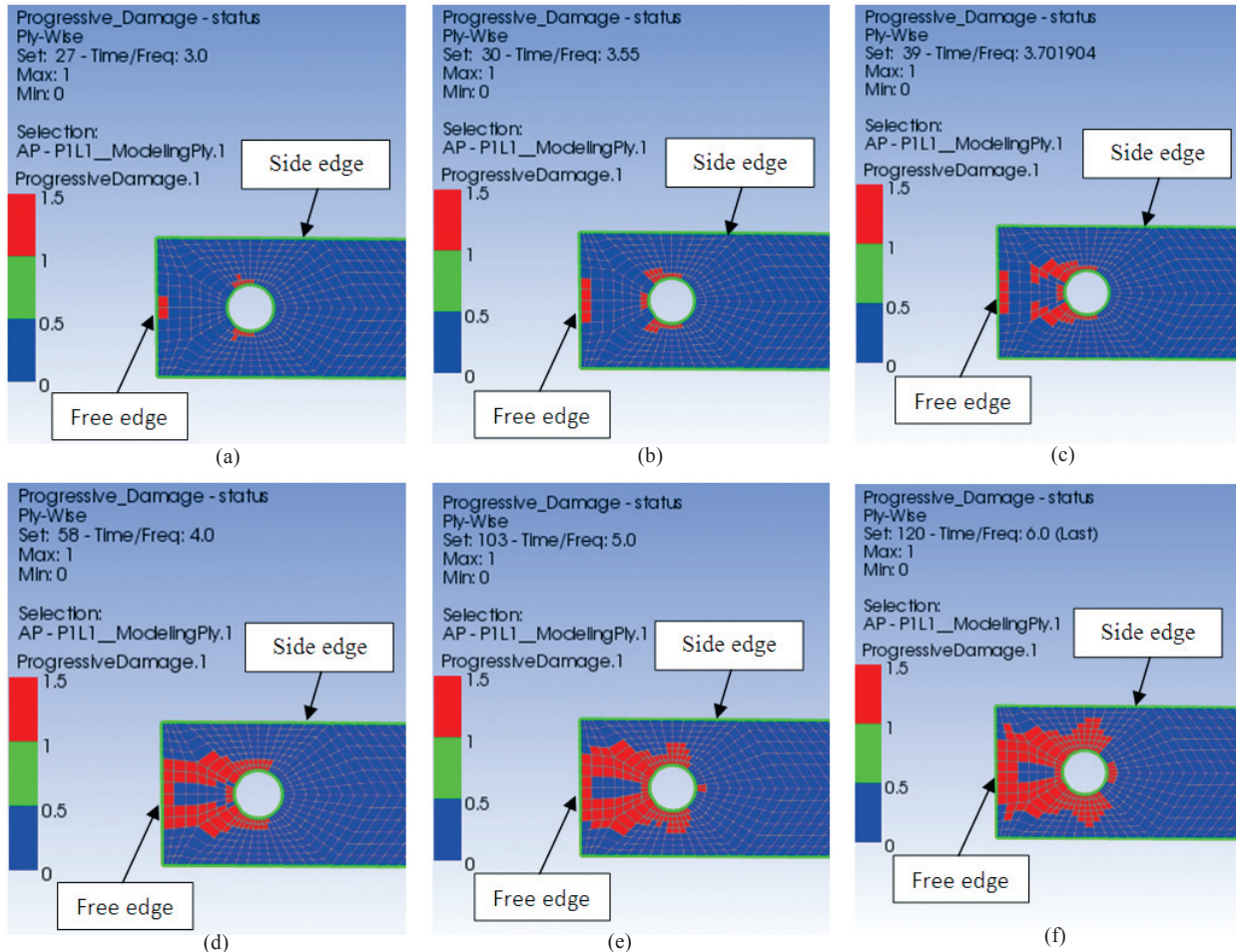


Figure 10. Progressive damage status under tensile load at different stages for E/D = 2 and W/D = 3 in the outer layer.

with large E/D and W/D ratios *i.e.*, $E/D \geq 4$ and $W/D \geq 3$, fail in bearing mode.

Figure 11 shows the progressive damage contour plots for the specimen having $E/D = 5$ and $W/D = 6$ for middle layer

the experimental results. The results shows the good agreement between each other for the different geometric parameters.

Thereafter, the numerical analysis was used to find the effect of the thickness of the metal insert on the strength of

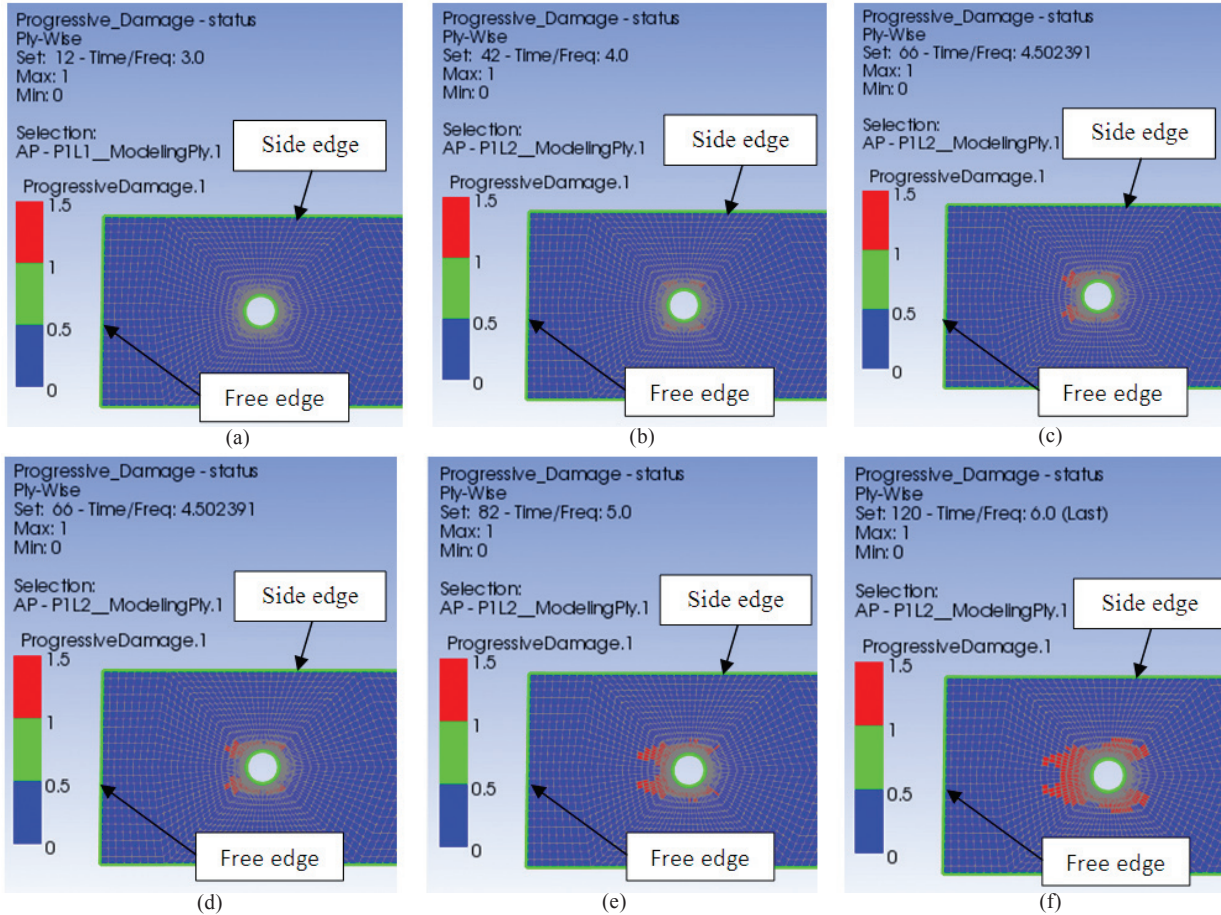


Figure 11. Progressive damage status under tensile load at different stages for $E/D = 5$ and $W/D = 6$ in the middle layer.

i.e., layers at 90° orientations with respect to the applied tensile load. It is observed from the figure that the failure begins around the hole surface towards side edge and then propagates towards free edge. Representing the pure bearing failure, damage does not reach upto the free edge of the specimen.

Figure 12 shows numerical failure loads for composite specimens with and without the metal inserts. The effect of E/D and W/D ratios on the failure load is clearly visible in the plots. The failure load increases with increase in E/D and W/D ratios. Use of metal inserts has clearly shown increase in first (middle ply) and last (outer ply) failure loads.

In general, last failure loads are significantly large than the first failure load. This confirms the mechanics behind the composite layer by layer structure, which tells that failure in middle layer which is at 90° to the applied load, occurs because of matrix failure and is basically due to the compressive force applied by the pin on the matrix, whereas failure in outer layers, aligned with the applied loads, are due to the tensile fiber failure and have large failure load values in comparison to the middle ply failure.

Figure 13 shows the comparison of the numerical with

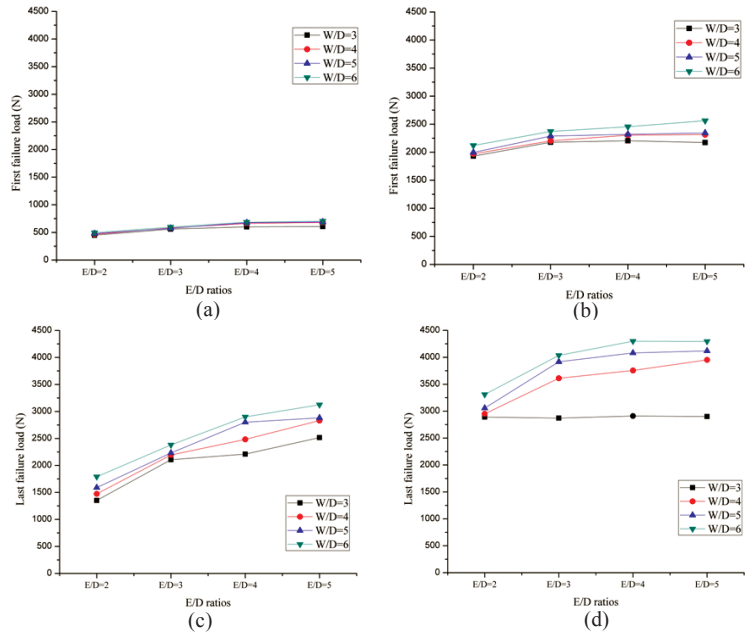


Figure 12. Failure loads for different specimen from numerical analysis: (a) First failure load without insert, (b) First failure load with insert, (c) Last failure load without insert, and (d) Last failure load with insert.

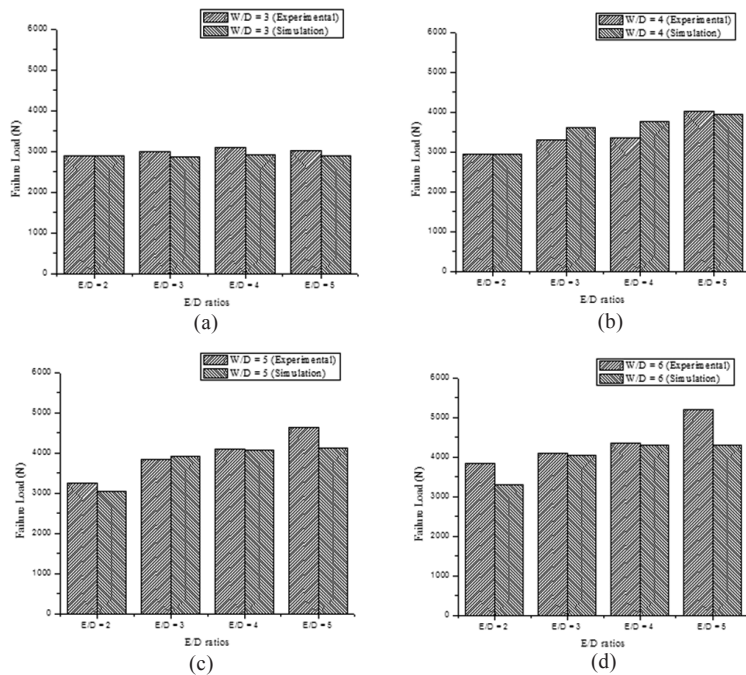


Figure 13. Comparison of experimental and numerical results: (a)W/D = 3, (b) W/D = 4, (c) W/D = 5, and(d) W/D = 6.

the joint. The analysis was done for the highest configuration of geometric parameters *i.e.*, E/D and W/D to be 5 and 6, respectively. Outer diameter of the metal insert was varied from 6 mm to 8 mm with an increment of 0.25 mm. The failure of the specimens with the variation of the insert thickness are shown in Fig. 14. It can be seen from Fig. 14, that the failure load of the specimens increases with increase in thickness of the insert but upto the outer diameter of 7.25 mm for the said configuration for first failure load. Beyond this value, the failure load decreases due to the reason that the distance between the hole and the side edge decreases leading to the net-tension failure mode. For the said configuration, the ideal thickness of the metal insert is 1.625 mm. The ideal thickness will vary as per the geometric configuration of the pin joint.

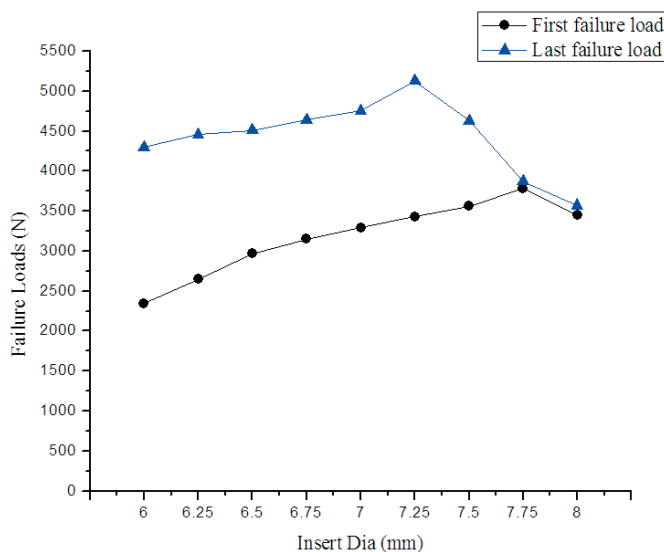


Figure 14. Failure loads for different metal insert thickness.

5. CONCLUSIONS

The present work deals with the effect of the metal inserts on the strength of the pin joints. Based on the results, the following conclusions have been drawn:

- Metal inserts reduce the stress concentration around the hole and redistribute the stresses around the pin/hole interface and significantly increase the failure load of the pin joint. The load increases in the range of 68 per cent to 90 per cent for different geometric configurations of the pin joints.
- Use of metal insert for $W/D \leq 3$ is not recommended as the failure is in net-tension mode which is the most fatal and undesired failure mode. It is due to the lesser distance between the insert and the side edge of the specimen.
- The failure load increases with increase in E/D and W/D ratios. There is bearing failure mode for E/D ratio ≥ 4 and W/D ratio ≥ 4 . Bearing failure mode has less serious consequences as compared to the net-tension and shear-out failure modes.
- The failure load of the specimens increases with increase in thickness of the insert but up to a certain value, beyond which the failure load decreases. For E/D and W/D to be 5 and 6, respectively, the ideal thickness of the metal insert is 1.625 mm. The ideal thickness will vary as per the geometric configuration of the pin joint.
- Progressive failure analysis along with the Hashin failure criterion was used to analyse the joints. The numerical results had a good agreement with the experimental results.

REFERENCES

1. Nilsson, S. Increasing strength of graphite/epoxy bolted joints by introducing an adhesively bonded metallic insert. *J. Compos. Mater.*, 1989, **23**, 642-650. doi: 10.1177/002199838902300701
2. Herrera-Franco, P.J. & Cloud, G.L. Strain-relief inserts for composite fasteners-an experimental study. *J. Compos. Mater.*, 1992, **26**, 751-768. doi: 10.1177/002199839202600506
3. Rispler, A.R.; Steven, G.P. & Tong, L. Photoelastic evaluation of metallic inserts of optimised shape. *Compos. Sci. Technol.*, 2000, **60**, 95-106. doi: 10.1016/S0266-3538(99)00107-4
4. Camanho, P.P. & Matthews, F. L. Bonded metallic inserts for bolted joints in composite laminates. *J. Mater.: Design Appl.*, 2000, **214**, 33-40. doi: 10.1177/146442070021400105
5. Camanho, P.P.; Tavares, C.; De Oliveira, R.; Marques, A. & Ferreira A. Increasing the efficiency of composite single-shear lap joints using bonded inserts. *Compos. Part B: Eng.*, 2005, **36**, 372-383. doi:10.1016/j.compositesb.2005.01.007
6. Karakuzu, R.; Gulem, T. & Icten, B.M. Failure analysis of woven laminated glass-vinylester composites with pin-loaded hole. *Compos. Struct.*, 2006, **72**, 27-32. doi:10.1016/j.compstruct.2004.10.009

7. Icten, B.M.; Karakuzu, R. & Toygar, M. E. Failure analysis of woven kevlar fiber reinforced epoxy composites pinned joints. *Compos. Struct.*, 2006, **73**, 443-450. doi:10.1016/j.compstruct.2005.02.016
8. Baba, B.O. Behavior of pin-loaded laminated composites. *Exp. Mech.*, 2006, **46**, 589-600. doi:10.1007/s11340-006-8735-z
9. Karakuzu, R.; Taylak, N.; Icten, B.M. & Aktas, M. Effects of geometric parameters on failure behavior in laminated composite plates with two parallel pin-loaded holes. *Composm Structm*, 2008, **85**, 1-9. doi:10.1016/j.compstruct.2007.10.003
10. Karakuzu, R.; Caliskan, C.R.; Aktas, M. & Icten, B.M. Failure behavior of laminated composite plates with two serial pin-loaded holes. *Compos. Struct.*, 2008, **82**, 225-234. doi:10.1016/j.compstruct.2007.01.002
11. Atas, C. Bearing strength of pinned joints in woven fabric composites with small weaving angles. *Compos. Struct.*, 2009, **88**, 40-45. doi:10.1016/j.compstruct.2008.04.002
12. Kishore, A.N.; Malhotra, S.K. & Prasad, N.S. Failure analysis of multi-pin joints in glass fibre/epoxy composite laminates. *Compos. Struct.*, 2009, **91**, 266-277. doi:10.1016/j.compstruct.2009.04.043
13. Aktas, A.; Imrek, H. & Cunedioğlu, Y. Experimental and numerical failure analysis of pinned-joints in composite materials. *Compos. Struct.*, 2009, **89**, 459-466. doi:10.1016/j.compstruct.2008.09.009
14. Asi, O. Effect of different woven linear densities on the bearing strength behaviour of glass fiber reinforced epoxy composites pinned joints. *Compos. Struct.*, 2009, **90**, 43-52. doi:10.1016/j.compstruct.2009.01.007
15. Asi, O. An experimental study on the bearing strength behavior of Al₂O₃ particle filled glass fiber reinforced epoxy composites pinned joints. *Compos. Struct.*, 2010, **92**, 354-363. doi:10.1016/j.compstruct.2009.08.014
16. Karakuzu, R.; Demirgoren, O.; Icten, B. M. & Deniz, M. E. Failure behavior of quasi-isotropic laminates with three-pin loaded holes. *Materials Design*, 2010, **31**, 3029-3032. doi:10.1016/j.matdes.2009.12.024
17. Turan, K.; Gur, M. & Kaman, M.O. Progressive failure analysis of pin-loaded unidirectional carbon-epoxy laminated composites. *Mech. Adv. Mater. Struct.*, 2014, **21**, 98-106. doi: 10.1080/15376494.2012.677109
18. Mara, V.; Haghani, R. & Al-Emrani, M. Improving the performance of bolted joints in composite structures using metal inserts. *J. Compos. Mater.*, 2016, **50**, 3001-3018. doi: 10.1177/0021998315615204.
19. Singh, M.; Saini, J.; Bhunia, H.; & Singh, P. Application of Taguchi method in the optimization of geometric parameters for double pin joint configurations made from glass-epoxy nanoclay laminates. *J. Compos. Mater.*, 2017, **51**, 2689-2706. doi: 10.1177/0021998316678920
20. Singh, M.; Bhunia, H. & Saini, J. Effect of ply orientation on strength and failure mode of pin jointed unidirectional glass-epoxy nanoclay laminates. *Def. Sci. J.*, 2015, **65**, 489-499. doi: 10.14429/dsj.65.8917
21. Hashin, Z. Failure criteria for unidirectional fiber composite. *J Appl. Mech.*, 1980, **47**, 329-334. doi:10.1115/1.3153664.

ACKNOWLEDGEMENTS

Thanks are due to Owens Corning India Pvt. Ltd. and Atul Ltd., Gujarat, India, who have provided the materials for the present work. The authors are also thankful to the reviewers for their comments which improved the manuscript.

CONTRIBUTORS

Mr Kulwinder Singh is PG in Computer Aided Design and Manufacturing Engineering from Thapar University, Patiala, Punjab. Currently pursuing his PhD from Thapar University, Patiala, Punjab. His research work involves analysis of mechanical joints prepared from polymer nanocomposite materials. In the current study, he is involved in the literature review, preparation of laminates, preparation of mechanical joints, experimental testing and analysis using finite element methods.

Dr J.S. Saini is working as Associate Professor in Mechanical Engineering Department at Thapar University, Patiala, Punjab. His specialisation is design and analysis. He has nearly 25 research papers in various journals and conferences. Presently he is working in the area of nano composites and their analysis. In the current study, he is involved in literature review, testing of the mechanical joints and analysis of the results.

Dr H. Bhunia is working as Professor in Chemical Engineering Department at Thapar University, Patiala, Punjab. His specialisation is polymer nano composites. He has published nearly 60 research papers and three books. In the current study, he is involved in material selection, purchasing of material and preparation of glass fiber reinforced laminates.